MOX–Report No. 11/2010

Controlled release with finite dissolution rate

Paolo Biscari, Sara Minisini, Dario Pierotti,
Gianmaria Verzini, Paolo Zunino

MOX, Dipartimento di Matematica "F. Brioschi"
Politecnico di Milano, Via Bonardi 9 - 20133 Milano (Italy)

mox@mate.polimi.it http://mox.polimi.it

Controlled release with finite dissolution rate*

Paolo Biscari[◇], Sara Minisini[♯], Dario Pierotti[◇], Gianmaria Verzini[◇], Paolo Zunino[♯].

April 7, 2010

[◇] Dipartimento di Matematica "F. Brioschi", Politecnico di Milano
Piazza Leonardo da Vinci 32, 20133 Milano, Italy
paolo.biscari@polimi.it, dario.pierotti@polimi.it,
gianmaria.verzini@polimi.it

[♯] MOX– Modellistica e Calcolo Scientifico
Dipartimento di Matematica "F. Brioschi", Politecnico di Milano
Piazza Leonardo da Vinci 32, 20133 Milano, Italy
sara.minisini@polimi.it, paolo.zunino@polimi.it

Keywords: reaction-diffusion equations, coated stent, medical applications, asymptotic behavior of solutions, numerical simulation

Abstract

We consider a two-phase generalization of the classical Higuchi's model for controlled drug release. The drug is assumed to be prepared in a drug eluting stent in its solid phase by immersion in a polymeric matrix which eventually delivers the drug when it reaches the free end. We derive a single effective evolution equation, which we prove to be equivalent to the original system of two coupled PDE's. We provide analytical estimates for the asymptotic regimes of large and small diffusion. Results from numerical simulations allow then to fill up the gap, and understand the behavior of the system in intermediate regimes.

1 Introduction

Drug release from matrix substrates has been extensively studied from both the theoretical and the applicative points of view [14]. The main technological challenge that has motivated such efforts is to design a substrate that guarantees

*S.M. and P.Z. were supported by the Grant *Nanobiotechnology: Models and methods for degradable materials* of the Italian Institute of Technology (IIT) and by the European Research Council Advanced Grant *Mathcard, Mathematical Modelling and Simulation of the Cardiovascular System*, Project ERC-2008-AdG 227058.

a desired (or controlled) drug release profile [13]. This is achieved by suitably tuning the drug dissolution and diffusion properties into the substrate.

In this paper we address the problem from the point of view of mass transport rather than material science. In particular, we will focus on how dissolution and diffusion phenomena influence the drug release rate from a slab with constant and uniform physical properties. Nevertheless, the interplay between drug and substrate is another area of controlled drug release studies, which is particularly interesting when the substrate is a polymer matrix. For a few recent examples of this analysis we refer to [15, 16].

The development and analysis of mathematical models for controlled drug release is a vivid field of research. A milestone in this field is the work by Higuchi [11, 12], where a one-phase, moving-boundary model is proposed to study drug release from a substrate loaded with a uniform initial concentration. An analytical explicit solution is derived under suitable simplifications such as the assumption that the dissolution is instantaneous and that the substrate can be subdivided in two regions, one where all the drug is dissolved, and the other where dissolved drug is in equilibrium with solid drug, and hence dissolved drug concentration is constant. Numerous generalizations of this model have been proposed with the aim to progressively remove these restrictive assumptions. We refer to [14] for an overview.

To the best of our knowledge, the most advanced description of dissolution controlled drug release is provided by Frenning in [7, 8]. It consist of a two phase model (solid and dissolved drug) for drug dissolution and diffusion accounting for a finite dissolution rate. In particular, we refer here to the simpler case [7] where dissolved drug does not interact with the substrate. More precisely, we consider the following problem

$$\begin{cases} \partial_\tau C - D\partial_{yy} C = A(S^+)^{2/3}(c_s - C) \quad 0 < y < b,\ 0 < \tau < T' \\ \partial_\tau S = -A(S^+)^{2/3}(c_s - C) \\ C(y,0) = 0, \quad S(y,0) = \sigma c_s \\ C_y(0,\tau) = 0, \quad C(b,\tau) = 0, \end{cases} \tag{1}$$

where (y, τ) respectively denote the space and time variables, $C = C(y, \tau)$ and $S = S(y, \tau)$ represent the drug concentrations in the dissolved and the solid phase, $c_s > 0$ is the saturation concentration for the dissolved drug, $D > 0$ is the diffusion coefficient, $A > 0$ is a (suitably dimensioned) reaction coefficient, and σ is a non-negative, dimensionless function describing the, possibly position-dependent, initial solid loading. Finally, $f^+ = \max\{f, 0\}$ denotes the positive part of a function f. The initial and boundary conditions are chosen such as to model the following physical situation. We assume that at the initial time all the drug is loaded in the solid phase, and thus $C(y, 0) = 0$ for all y. The extreme points of the substrate respectively represent an inert boundary at $y = 0$, where no drug is released, and a perfect washing condition at $y = b$, where the external medium is assumed to be able to wash out the drug at any time.

Starting from this point, we perform a detailed analysis of the model, aiming to determine lower-upper bounds and regularity of the solutions, as well as their asymptotic behaviors for small and large diffusion limits. In this respect, the present work can be considered as the extension of the analysis performed in [2] to a more general description of dissolution and diffusion.

From the applicative point of view, the present work may be useful for several biomedical applications. In particular, we refer to polymeric coated drug eluting stents (also called medicated stents), which are miniaturized metal structures coated with a micro-film containing drugs. After the implantation of the device into a specific vascular district, typically a location of the coronary arteries, the drug is locally released into the cardiovascular system for healing purposes. In particular, the present work could provide useful tools to complement more detailed computational models to design such devices, as the ones addressed in [6, 18, 3, 17].

We are, in particular, interested in providing estimates of quantities of applicative interest, such as the release rate. The validity of these estimates will be discussed, also resorting to numerical simulations. The plan of the paper is as follows. In Section 2 we show that the study of the differential system (1) is equivalent to a single partial differential equation, a remark which may prove to be quite useful in numerical simulations. Moreover, by means of the use of suitably adapted maximum principles (whose analytical technical details are collected in Appendix A), we prove some theoretical estimates on the solutions of (1). Section 3 is devoted to the study of the large-diffusion limit. Such limit may be studied through a regular perturbation scheme, and several analytical estimates are provided for both the solutions and the release rate. Section 4 is dedicated to the much more complicated small-diffusion limit. This is a singular perturbation problem, and the solutions possess a richer structure. Initial boundary layers are evidenced, travelling-wave solutions are identified, and their speed is computed as well. Throughout the analysis, the theoretical estimates are tested against numerical simulations. A concluding section collects the results and discusses the possible improvements that emerge from our analysis. Finally, Appendix B collects the details of the numerical simulations of the problem.

2 Adimensionalization and general properties of the solutions

It is the aim of this section to provide an equivalent formulation of the differential system (1) as a problem for a single unknown, for which we will establish existence and uniqueness of classical solutions. We then prove some estimates on the solutions, among which we highlight the existence of a finite and position-dependent *stopping time* such that the solid concentration is positive for times preceding the stopping time, and null thereafter.

Our first step is to adimensionalize the system (1), in order to evidence the existence of a single relevant dimensionless parameter, which governs the behavior of the solutions. We introduce the dimensionless spatial and time variables (x,t), unknown concentrations c, s, and diffusion α such that

$$x = \frac{y}{b}, \quad t = \frac{Ac_s^{2/3}\tau}{3}, \quad c(x,t) = \frac{C\big(bx, 3t/(Ac_s^{2/3})\big)}{c_s}, \quad s(x,t) = \frac{S\big(bx, 3t/(Ac_s^{2/3})\big)}{c_s},$$

and $\alpha = 3D/(b^2Ac_s^{2/3})$. As a result, we obtain that c, s satisfy the differential problem

$$\begin{cases} c_t - \alpha c_{xx} = 3(s^+)^{2/3}(1-c) & 0 < x < 1,\ 0 < t < T \\ s_t = -3(s^+)^{2/3}(1-c) & \\ c(x,0) = 0, \quad s(x,0) = \sigma(x) & \\ c_x(0,t) = 0, \quad c(1,t) = 0. & \end{cases} \tag{2}$$

In order to ease the presentation, we will often restrict to the case of uniform initial loading $\sigma(x) \equiv \sigma_0 > 0$, though we remark that almost all the results can be easily generalized to the non-uniform case.

2.1 A priori estimates

To start with, we use the maximum principle to derive some estimates on any (possible) solution.

Proposition 2.1 *Let (c,s) be a solution of (2), with σ a piecewise continuous function in $[0,1]$ such that $0 \le \sigma(x) \le \sigma_1$.*

Then, for every $t \ge 0$ and $0 \le x \le 1$, we have

$$0 \le c(x,t) \le 1 - \frac{\cosh \lambda x}{\cosh \lambda} \le 1 - \frac{1}{\cosh \lambda} < 1, \quad \textit{where} \quad \lambda = \sqrt{\frac{3\sigma_1^{2/3}}{\alpha}}. \tag{3}$$

Moreover, $0 \le s(x,t) \le \sigma(x)$ is a non-increasing function of time, and strictly decreasing whenever it is not null.

Finally, if σ is strictly positive in any subinterval in $[0,1]$, the equality $c(x,t) = 0$ holds only at the initial time $t = 0$, that is, the concentration c does never vanish at any point $x \neq 1$ and time, other than its requested initial condition.

Proof. Since $3(s^+)^{2/3} \ge 0$, the maximum principle (see Lemma A.1 in the Appendix) applied twice, first to the equation for c, and then to the trivially obtained equivalent equation for $(1-c)$, immediately yields $0 \le c(x,t) \le 1$ for all (x,t).

Let now λ be defined as in (3), and

$$d(x,t) = 1 - \frac{\cosh \lambda x}{\cosh \lambda}, \qquad x \in [0,1].$$

The function d is non-negative, and monotonically decreasing in x, with $0 = d(1) \leq d(x) \leq d(0) < 1$. By direct inspection it is easy to verify that it satisfies the partial differential equation

$$d_t - \alpha d_{xx} + 3\sigma_1^{2/3} d = 3\sigma_1^{2/3},$$

with $d_x(0,t) = 0$ and $d(1,t) = 0$. Furthermore it holds

$$(d-c)_t - \alpha(d-c)_{xx} + 3\sigma_1^{2/3}(d-c) = 3\left(\sigma_1^{2/3} - (s^+)^{2/3}\right)(1-c) \geq 0, \quad \text{with}$$
$$(d-c)\Big|_{(x,0)} \geq 0, \quad (d-c)_x\Big|_{(0,t)} = 0, \quad \text{and} \quad (d-c)\Big|_{(1,t)} = 0.$$

Then again the maximum principle applies to the function $(d-c)$ and we obtain, for every (x,t),

$$c(x,t) \leq d(x) \leq d(0) < 1,$$

that is an upper bound for c which proves that the drug concentration in the dissolved phase does never reach its saturation value. In turn, this implies that $s_t < 0$ when $s > 0$. Since $s \leq 0$ implies $s_t = 0$, we infer that s can not become negative, and the second claim follows.

Finally, the fact that c cannot vanish at any time (different from $t = 0$) follows from the strong maximum principle, and the observation that $c_t(x,0)$ is strictly positive whenever $\sigma(x) > 0$. □

By arguing as above, it is easy to show that, despite the lack of Lipschitz-continuity in the corresponding equation, for any fixed $c(x,t)$, there exists at most one solution of the Cauchy problem

$$s_t = -3(s^+)^{2/3}(1-c), \quad s(x,0) = \sigma(x).$$

Furthermore

$$s(x,t_0) = 0 \quad \Longrightarrow \quad s(x,t) = 0 \text{ whenever } t \geq t_0.$$

As we mentioned, existence, uniqueness, and much more information for system (2) will descend from an equivalent problem.

2.2 Equivalent problems

In this section we determine a single partial differential equation equivalent to the system (2). For the sake of brevity we initially consider a uniform initial datum $\sigma(x) \equiv \sigma_0 > 0$.

When $s(x,t) > 0$, the second equation in (2) can be rewritten as

$$\frac{1}{3}(s^+)^{-2/3} s_t = -(1-c) \tag{4}$$

which, once integrated in time, yields

$$(s^+(x,t))^{1/3} = \sigma_0^{1/3} - t + \int_0^t c(x,\tau)\, d\tau.$$

This suggests to introduce a new unknown in the form of the previous right hand side,

$$u(x,t) = \sigma_0^{1/3} - t + \int_0^t c(x,\tau)\, d\tau.$$

Formal computations then show that u is a solution of

$$\begin{cases} u_t - \alpha u_{xx} = \sigma_0 - 1 - (u^+)^3 & 0 < x < 1,\ 0 < t < T \\ u(x,0) = \sigma_0^{1/3} \\ u_x(0,t) = 0 \\ u(1,t) = \sigma_0^{1/3} - t. \end{cases} \tag{5}$$

As a consequence, it is natural to wonder whether (5) is (uniquely) solvable, and in such a case to prove that the relation between (c,s) and u is not only formal. In particular, we aim at understanding whether the relation holds once we remove the condition $s(x,t) > 0$. As one can easily see, the key point in this direction is to prove higher regularity for u (roughly speaking, existence and continuity of second and third derivatives, possibly up to some part of the boundary). This plan is successfully addressed in Appendix A, and allows us to obtain existence, uniqueness and the actual solution of (2) by integrating (5).

Proposition 2.2 *Let (c,s) be a classical solution of (2) (in particular, c is twice differentiable in the space variable, once in the time variable, and continuous up to the boundary), and*

$$u(x,t) = \sigma_0^{1/3} - t + \int_0^t c(x,\tau)\, d\tau.$$

Then $s(x,t) = (u^+(x,t))^3$, and u solves (5).

On the other hand, let u be (the unique) solution of (5). Then the pair

$$s(x,t) = \left(u^+(x,t)\right)^3, \qquad c(x,t) = 1 + u_t(x,t)$$

is (the unique) solution of (2).

Proof. As regards the first part, it is trivial to see that u (defined in terms of c) verifies the initial and boundary conditions. By assumption, the function $\varphi(x,t) = (u^+(x,t))^3$ is C^1 in time up to 0, and $\varphi \geq 0$, so that we obtain

$$\varphi_t = 3\left(u^+\right)^2 u_t = -3\left(\varphi^+\right)^{2/3}(1-c).$$

Since $\varphi(x,0) = \sigma_0$, the remark at the end of the previous subsection implies that $\varphi \equiv s$. Finally, since equation (2) implies $c_t - \alpha c_{xx} = -s_t$, by straightforward calculations we obtain

$$\alpha u_{xx} = \int_0^t \alpha c_{xx}(x,\tau)\, d\tau = \int_0^t (c_t + s_t)\, d\tau = c + s - \sigma_0,$$

and therefore

$$u_t - \alpha u_{xx} = \sigma_0 - 1 - s.$$

Recalling the relation between s and u, the first part of the proposition follows.

On the other hand, by Proposition A.1 there exists exactly one solution u of (5), and the functions u_t, u_x, u_{tx} u_{xx}, u_{xxx}, u_{tt}, and u_{txx} are continuous up to the boundary (possibly except for the point $(x,t) = (1,0)$). This allows us to check, by direct evaluation, that c, s satisfy (2). □

By reasoning as above, one can also obtain another equivalent formulation of the problem, where all the boundary conditions are homogeneous. Indeed, if we let

$$v(x,t) = \int_0^t c(x,\tau)\,d\tau, \quad \text{then} \quad s(x,t) = \left[\left(\sigma_0^{1/3} - t + v\right)^+\right]^3,$$

and

$$\begin{cases} v_t - \alpha v_{xx} = \sigma_0 - \left[\left(\sigma_0^{1/3} - t + v\right)^+\right]^3 & 0 < x < 1,\ 0 < t < T \\ v(x,0) = 0 \\ v_x(0,t) = 0 \\ v(1,t) = 0. \end{cases} \tag{6}$$

Equivalent formulations such as (5) or (6) can be determined also when the initial loading $\sigma(x)$ is not uniform. In fact, it is to be noted that in (6) we may simply replace σ_0 by a variable $\sigma(x)$, and all statements still hold. On the contrary, some extra-care is necessary if we want to generalize equation (5). In particular, such an equivalent problem can be easily obtained only if $\sigma^{1/3}$ is of class C^2. When this is the case, the partial differential equation in (5) is replaced by

$$u_t - \alpha(u - \sigma^{1/3})_{xx} = \sigma - 1 - (u^+)^3.$$

2.3 Stopping time

In the following we let c and s denote the unique solution of (2). We have already remarked that, because of the (parabolic) strong maximum principle, c can not vanish in finite time. On the other hand, as we are now going to show, the contrary happens for s. At points x such that $\sigma(x) = 0$, it is clear from $(2)_2$ that the unique solution satisfies $s(x,t) = 0$ for all t. If, on the contrary, $\sigma(x) > 0$, equation (4) and Proposition 2.1 ensure that, as long as $s(x,t) > 0$,

$$\frac{ds^{1/3}}{dt} = -(1-c) \le -(\cosh\lambda)^{-1}, \tag{7}$$

where $\lambda = \sqrt{3\sigma_1^{2/3}/\alpha}$, and σ_1 is an upper bound for σ. By integrating with respect to time we readily obtain that, as long as $s(x,t) > 0$ it holds

$$s(x,t) \le \left(\sigma^{1/3}(x) - (\cosh\lambda)^{-1}t\right)^3,$$

and therefore $s(x,t) = 0$ for $t \geq \sigma^{1/3}(x) \cosh \lambda$. Consequently we may define the *stopping time* as

$$T(x) = \sup\{\bar{t} : s(x,t) > 0 \text{ in } [0,\bar{t})\} = \inf\{\bar{t} : s(x,t) \equiv 0 \text{ in } [\bar{t}, +\infty)\}. \tag{8}$$

The function T is well defined, and bounded in $[0,1]$. The stopping time gives an important estimate of the time of drug delivery. In particular, before the time $T_{\min} = \inf_{x\in[0,1]} T(x)$ the solid drug is present in all the stent, while after a time $T_{\max} = \sup_{x\in[0,1]} T(x)$ all the drug is dissolved, and the subsequent evolution of the system is a simple diffusion process of the quantity $c(x,t)$. Clearly $T_{\min} = 0$, if $\sigma(x) = 0$ for some x. In fact, $T(x) = 0$ whenever $\sigma(x) = 0$.

It is our aim to prove next some general properties about the function $T(x)$. We will investigate its continuity and differentiability and, whenever possible, derive expressions for its derivatives $T'(x)$ and $T''(x)$. Moreover we will show that, under suitable hypotheses for σ, T is monotonically decreasing, so that in particular $T_{\max} = T(0)$, and $T_{\min} = T(1)$. Incidentally, we note that, because of the boundary condition $c(1,t) = 0$, equation (7) implies

$$s(1,t) = \left[\left(\sigma^{1/3}(1) - t\right)^+\right]^3 \quad \forall t \geq 0 \quad \Longrightarrow \quad T(1) = \sigma^{1/3}(1).$$

Let us consider an $x \in [0,1]$ such that $\sigma(x) > 0$. Then, equation (7) holds at that x for all $t \in [0, T(x))$. A direct integration provides then

$$\sigma^{1/3}(x) - s^{1/3}(x,t) = \int_0^t (1 - c(x,\tau))\, d\tau \quad \forall t \in [0, T(x)). \tag{9}$$

All the quantities in (9) are continuous in the time variable when $t \to T(x)$. By taking the limit, and considering that $s(x, T(x)) = 0$, we obtain

$$\int_0^{T(x)} (1 - c(x,\tau))\, d\tau = \sigma^{1/3}(x). \tag{10}$$

Equation (10) defines implicitly $T(x)$ whenever $\sigma(x) > 0$. Since c is at least of class C^2 with respect to x, the implicit function theorem ensures that T is at least twice-differentiable whenever σ is so (in addition to being not null). On the other hand, T exhibits jump discontinuities whenever σ does. More explicitly we have

$$\big(1 - c(x,T(x))\big)T'(x) - \int_0^{T(x)} c_x(x,\tau)\, d\tau = \frac{d\sigma^{1/3}}{dx} \tag{11}$$

and

$$\begin{aligned}\big(1 - c(x,T(x))\big)T''(x) - \big(2c_x(x,T(x)) + c_t(x,T(x))T'(x)\big)T'(x) \\ - \int_0^{T(x)} c_{xx}(x,\tau)\, d\tau = \frac{d^2\sigma^{1/3}}{dx^2}.\end{aligned} \tag{12}$$

We remark that equation (11) implies

$$T'(0) = \frac{\sigma^{-2/3}(0)\sigma'(0)}{3\big(1 - c(0, T(0))\big)}$$

so that, in particular, $T'(0)$ shares the sign with $\sigma'(0)$.

We conclude this section by proving that T is monotonically decreasing for a wide class of initial loadings σ, including all uniform loadings with $\sigma(x) \equiv \sigma_0 \geq 1$.

Proposition 2.3 *Let $T(x)$ be the stopping time defined in (8), and let the initial loading $\sigma(x)$ satisfy the following properties:*

- *$\sigma \in C^2([0, a])$ for some $a \in (0, 1]$, and $\sigma(x) \geq 1$ for all $x \in [0, a]$.*
- *$\sigma'(0) \leq 0$, and $d^2(\sigma^{1/3})/dx^2 \leq 0$ for all $x \in [0, a]$.*

Then T is strictly monotonically decreasing in $[0, a]$.

Proof. We begin by showing that all critical points of $T(x)$ in $[0, a]$ are necessarily local isolated maxima. Assume that $x^* \in [0, a]$ be such that $T'(x^*) = 0$. Then, equation (12) implies

$$\begin{aligned}
\big(1 - c(x^*, T(x^*))\big)T''(x^*) &= \int_0^{T(x^*)} c_{xx}(x^*, \tau)\, d\tau + \frac{d^2\sigma^{1/3}}{dx^2}(x^*) \\
&= \frac{1}{\alpha}\int_0^{T(x^*)} \big(s_t + c_t\big)\, d\tau + \frac{d^2\sigma^{1/3}}{dx^2}(x^*) \\
&= \frac{1}{\alpha}\big(c(x^*, T(x^*)) - \sigma(x^*)\big) + \frac{d^2\sigma^{1/3}}{dx^2}(x^*) < 0,
\end{aligned}$$

therefore $T''(x^*) < 0$ and T has a local isolated maximum in x^*. Since this holds for every critical point of T, and $T'(0) \leq 0$ because of the condition on $\sigma'(0)$, we obtain that T is strictly decreasing in $x \in [0, a]$. □

Table 1 tests our analytical estimates for $T_{\max} = T(0)$ in the case of uniform loading, with $\sigma(x) \equiv \sigma_0 = 3$, for different values of the dimensionless parameter α. With such a choice for σ, the parameter a can be chosen equal to 1, and it holds

$$T_{\min} = T(1) = \sigma_0^{1/3} < T(x) < T_{\max} = T(0) \leq \sigma_0^{1/3}\cosh\lambda \quad \forall x \in (0, 1). \tag{13}$$

It turns out that the bound is rather sharp in the large diffusion limit, while it yields a diverging overestimate in the small diffusion limit. The next sections will help us in understanding this behavior.

3 Large diffusion

We are now ready to derive an asymptotic expansion fit to describe the behavior of the solutions of system (2) in the large diffusion limit, that is when

$$\alpha = \frac{3D}{b^2 A c_s^{2/3}} \gg 1 \quad \Longleftrightarrow \quad D \gg b^2 A c_s^{2/3}\,.$$

α	D (mm^2/s)	$\sigma_0^{1/3}\cosh\lambda$	$T_{\max}$
4.7×10^{-3}	10^{-10}	$1.\times10^{15}$	$4.\times10^{2}$
4.7	10^{-7}	2.50	1.76
4.7×10^{4}	10^{-3}	1.442	1.442

Table 1: Comparison of the analytical bound for the maximum stopping time $T_{\max}$ and the results of the numerical simulations. The values of the dimensionless parameter α have been obtained from the corresponding values of D by choosing the physiologically sensible values $A = 10^{-4}$ (mg/mm^3)$^{-2/3}$/s, $b = 20\times10^{-3}$mm, and $c_s = 2$mg/mm^3.

When this is the case, the release/delivery process is dominated by the diffusion, which immediately washes out the drug dissolved within the stent. Consequently, we seek for solutions which might be expanded in powers of the small quantity α^{-1}. More precisely we set

$$c(x,t) = \alpha^{-1}c_1(x,t) + o(\alpha^{-1}) \quad \text{and} \quad s(x,t) = s_0(x,t) + \alpha^{-1}s_1(x,t) + o(\alpha^{-1}).$$

3.1 Initial times

Let us initially consider a uniform initial loading $\sigma(x) \equiv \sigma_0$. Let $t = \hat{t}/\alpha$. (Note that $\hat{t}$ is here assumed to be finite, so that we are inspecting the very initial time evolution of the solutions.) Then $d/(dt) = \alpha\, d/(d\hat{t})$, and the leading contributions to system (2) are given by

$$c_{1,\hat{t}} - c_{1,xx} = 3(s_0^+)^{2/3} \quad \text{and} \quad s_{0,\hat{t}} = 0.$$

The second equation indicates that, in this very fast regime, the variable s does not evolve:

$$s_0(x,\hat{t}) = \sigma_0.$$

On the contrary, the first equation yields a very fast evolution for the concentration, which quickly evolves towards its stationary (in $\hat{t}$) solution

$$\lim_{\hat{t}\to+\infty} c_1(x,\hat{t}) = \frac{3}{2}\,\sigma_0^{2/3}\big(1-x^2\big).$$

3.2 Finite times

In finite times, the leading contribution to the evolution of the variable s can be directly integrated:

$$s_{0,t} = -3(s_0^+)^{2/3} \quad \Rightarrow \quad s_0(x,t) = \begin{cases} \left(\sigma_0^{1/3} - t\right)^3 & \text{if } t \le \sigma_0^{1/3} \\ 0 & \text{if } t > \sigma_0^{1/3}. \end{cases}$$

Consequently, and since $c_{1,xx} = -3(s_0^+)^{2/3} = s_{0,t}$, we obtain

$$c_1(x,t) = \begin{cases} \frac{3}{2}\left(\sigma_0^{1/3} - t\right)^2\left(1 - x^2\right) & \text{if } t \le \sigma_0^{1/3} \\ 0 & \text{if } t > \sigma_0^{1/3}. \end{cases} \tag{14}$$

Note that $\lim_{t\to 0} c_1(x,t) = \lim_{\hat{t}\to+\infty} c_1(x,\hat{t}) \neq 0$, while $\lim_{\hat{t}\to 0} c_1(x,\hat{t}) = 0$ for any $x \in [0,1]$.

3.3 Stopping time

The 0-th order solution for s yields a constant stopping time $T_0(x) \equiv \sigma_0^{1/3}$. Let us now compute the first correction to the stopping time, due to the effect of the perturbation of s. The $O(\alpha^{-1})$ contribution to the evolution equation for s is determined by the ordinary differential equation (in which x plays the role of a parameter)

$$s_0^{1/3} s_{1,t} + 2s_1 = 3s_0 c_1 \quad \text{for} \quad t < \sigma_0^{1/3},$$

and the $O(\alpha^{-1})$ approximation to s is given by

$$s_0 + \alpha^{-1} s_1 = \begin{cases} \left(\sigma_0^{1/3} - t\right)^3 + \frac{3}{2}\,\alpha^{-1}(\sigma_0^{1/3} - t)^2(1-x^2)\left(\sigma_0 - (\sigma_0^{1/3} - t)^3\right) & \text{if } t \le \sigma_0^{1/3} \\ 0 & \text{if } t > \sigma_0^{1/3}. \end{cases}$$

Note that, up to this order, the stopping time remains $T_0(x) \equiv \sigma_0^{1/3}$.

If we proceed further in the expansion, we find that

$$s(x, \sigma_0^{1/3}) = \frac{1}{8}\alpha^{-3}\sigma_0^3(1-x^2)^3 + o(\alpha^{-3}),$$

so that

$$T_0(x) = \sigma_0^{1/3} + \tfrac{1}{2}\alpha^{-1}\sigma_0(1-x^2) + o(\alpha^{-1}). \tag{15}$$

3.4 Release rate

The release rate of the drug is defined as the rate at which the drug abandons the substrate. In view of equation (2), it is controlled by $c_x(1,t)$, since

$$R(t) := -\frac{d}{dt}\int_0^1 (c+s)\,dx = -\int_0^1 \alpha c_{xx}(x,t)\,dx = -\alpha\, c_x(1,t).$$

By using equation (14) we may derive the $O(1)$ approximation to the release rate:

$$R_0(t) = -\alpha c_{1,x}(1,t) = \begin{cases} 3\big(\sigma_0^{1/3} - t\big)^2 & \text{if } t \le \sigma_0^{1/3} \\ 0 & \text{if } t > \sigma_0^{1/3}, \end{cases}$$

where $R(t) = R_0(t) + O(\alpha^{-1})$.

3.5 Variable initial distribution

Let us now consider the case in which $s(x,0) = \sigma(x)$. At leading order, we still obtain $s_0(x,\hat{t}) = \sigma(x)$, while the fast evolution of the concentration leads to

$$\lim_{\hat{t}\to+\infty} c_1(x,\hat{t}) = 3\int_x^1 \left(\int_0^z \sigma^{2/3}(z')\,dz'\right) dz.$$

In finite times, the leading contribution to the evolution of the variable s can still be directly integrated:

$$s_{0,t} = -3(s_0^+)^{2/3} \quad \Rightarrow \quad s_0(x,t) = \begin{cases} \big(\sigma^{1/3}(x) - t\big)^3 & \text{if } t \le T_0(x) \\ 0 & \text{if } t > T_0(x), \end{cases}$$

where now the stopping time depends on x even at its leading order: $T_0(x) = \sigma^{1/3}(x) + O(\alpha^{-1})$. Moreover,

$$c_1(x,t) = 3\int_x^1 \left(\int_0^z s_0^{2/3}(z',t)\,dz'\right) dz.$$

The release rate is thus $R(t) = R_0(t) + O(\alpha^{-1})$, with

$$R_0(t) = -\alpha c_{1x}(1,t) = 3\int_0^1 s_0^{2/3}(u,t)\,du = 3\int_0^1 \Big[\big(\sigma^{1/3}(u) - t\big)^+\Big]^2\,du. \tag{16}$$

It is worth to be noticed that, even in this simple case, equation (16) shows that it is possible to control the time-dependent release rate with the spatial initial drug distribution. However, equation (16) shows that, in the large-diffusion limit, the release rate is a monotonically decreasing function of time.

The behavior of the solution $c(x,t)$ and $s(x,t)$ in the large diffusion limit is illustrated in Figure 1. In particular, it shows the numerical approximation of the concentration profiles of $c(x,t)$ (left) and $s(x,t)$ (right) for $\alpha = 4.7 \times 10^4$, corresponding to $D = 10^{-3}\text{mm}^2/\text{s}$, the values of A, b, and c_s indicated in Table 1, and a uniform initial loading with $\sigma_0 = 3$. The sequence of curves correspond to a sequence of equidistributed time samples. Such plots support the results of Section 3.2 where the leading contribution of variable s is a constant function with respect to x and a decreasing function with respect to t. A similar conclusion can be driven by comparing the plots of concentration c with equation (14).

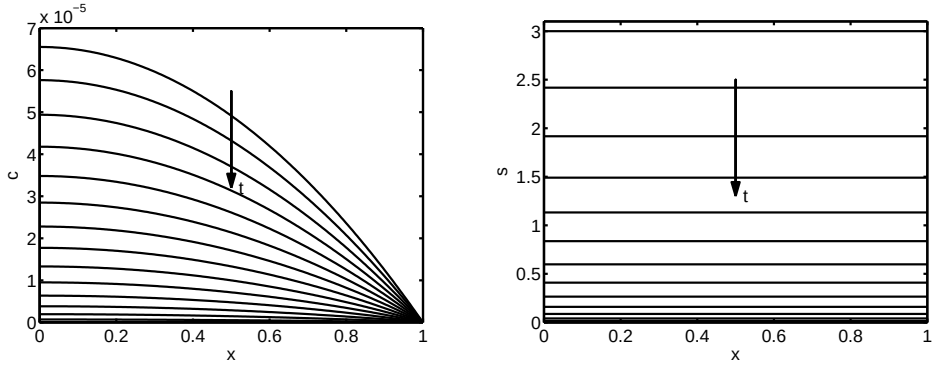

Figure 1: Numerical approximation of the concentration profiles of $c(x,t)$ (left) and $s(x,t)$ (right) for $\alpha = 4.7 \times 10^4$, and $\sigma(x) \equiv \sigma_0 = 3$.

4 Small diffusion

We now consider the case in which α is small. The behavior of the solution is now much more complex if compared with the case of α large. It will emerge, in particular, that the asymptotic behavior of the solutions follows from the analysis of a singular perturbation scheme.

4.1 Initial times

In the spirit of the last section, we first focus on the case of uniform initial loading, with the extra assumption that $\sigma(x) \equiv \sigma_0 > 1$. More general cases will be considered at the end of this section. In this limit, the diffusion effects arise in times of order α^{-1}, as we will show below. In time scales of $O(1)$, the only evolution that occurs is that, at each $x \in [0,1)$, the drug is melted from the solid to the liquid phase, until the concentration approaches its saturation limit $c_{\rm sat} = 1$ (while, consequently, s approaches the value $s_{\rm sat} = \sigma_0 - 1$). Such a saturation process is clearly hindered at $x = 1$, where the boundary condition $c = 0$ holds at all times. A boundary layer is thus to be expected close to the extreme $x = 1$. Away from this boundary layer, the initial time evolution can be analytically determined in an implicit form. It satisfies the differential problem

$$\begin{cases} c_{{\rm in},t} = 3(s_{\rm in}^+)^{2/3}(1 - c_{\rm in}) & 0 < x < 1 \\ s_{{\rm in},t} = -3(s_{\rm in}^+)^{2/3}(1 - c_{\rm in}) & \\ c_{\rm in}(x,0) = 0, \quad s_{\rm in}(x,0) = \sigma_0. & \end{cases} \tag{17}$$

The solution of (17) satisfies

$$\lim_{t\to\infty} s_{\rm in}(t) = s_{\rm sat} = \sigma_0 - 1 \quad \text{and} \quad \lim_{t\to\infty} c_{\rm in}(t) = c_{\rm sat} = 1. \tag{18}$$

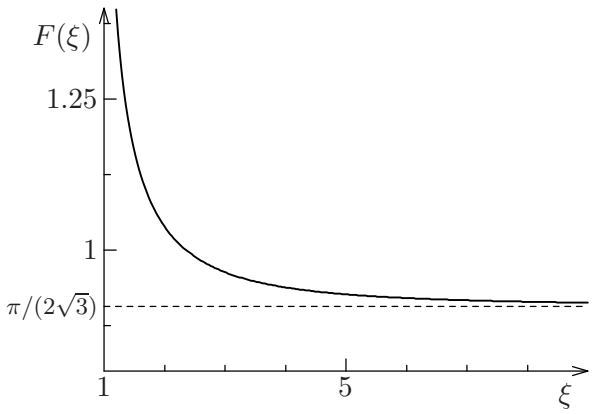

Figure 2: Plot of the function F defined in equation (19).

Indeed, the implicit solution of (17) can be written as $F(\xi(t)) - F(\xi_0) = \mu t$, where

$$F(\xi) = \frac{1}{\sqrt{3}} \arctan \frac{2\xi(t)+1}{\sqrt{3}} - \frac{1}{6} \log \frac{(\xi(t)-1)^2}{\xi(t)^2+\xi(t)+1}, \tag{19}$$

$\mu = (\sigma_0 - 1)^{2/3}$ is a positive parameter, and

$$s_{\text{in}}(t) = \mu^{3/2}\xi(t)^3, \qquad c_{\text{in}}(t) = \sigma_0 - s_{\text{in}}(t), \quad \text{with} \quad \xi_0 = \frac{(1+\mu^{3/2})^{1/3}}{\sqrt{\mu}}.$$

Figure 2 illustrates the behavior of the function defined in (19). As time increases, ξ decreases monotonically towards its asymptotic value $\lim_{t\to\infty} \xi(t) = 1$, which implies (18).

4.2 The initial boundary layer

While the melting occurs, a boundary layer appears close to the extreme $x = 1$, to ensure that the boundary condition $c(1,t) = 0$ is satisfied at all times. The asymptotic shape of this boundary layer, that is, the shape when the melting transient is completed, can be analytically estimated as well. Indeed, in this regime we may neglect the time derivative and solve the ordinary differential equation (in the variable x)

$$-\alpha c_{xx} = -3(\sigma_0 - c)^{2/3}(1-c), \tag{20}$$

where, by neglecting diffusion processes which occur at longer time scales, we have set $s = \sigma_0 - c$. Equation (20) can be analytically integrated once to yield

$$\alpha c_x^2 = \frac{9}{20}\left(3(\sigma_0-1)^{8/3} + (8-5c-3\sigma_0)(\sigma_0-c)^{5/3}\right),$$

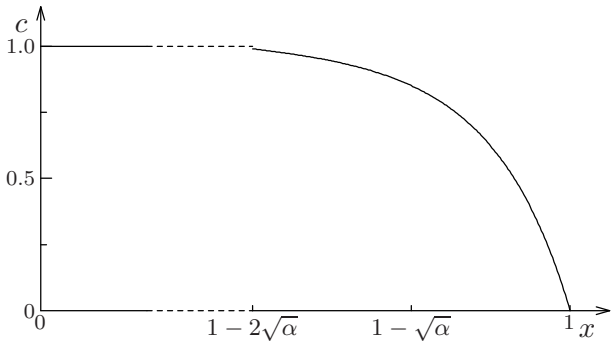

Figure 3: Plot of the function c obtained by gluing the outer solution $c_{\text{out}} = 1$, and the inner solution obtained by solving $\hat{c}'' = 3(\sigma_0 - \hat{c})^{2/3}(1 - \hat{c})$ with the boundary conditions indicated in the text. The dimensionless parameter σ_0 has been set equal to 3.

so that the release rate is given by

$$R(t) = -\alpha c_x\big|_{x=1} = \frac{3\sqrt{\alpha}}{2\sqrt{5}}\sqrt{3(\sigma_0 - 1)^{8/3} + (8 - 3\sigma_0)\sigma_0^{5/3}}.$$

An explicit analytical solution of equation (20) cannot be derived. Nevertheless, we may obtain some important information about the behavior of solutions in the small-α limit. The *outer* solutions, that is, the solutions of the (algebraic) equation obtained by setting $\alpha = 0$ in (20), must be constant, and equal to either σ_0 or 1. Since the first possibility is ruled out by the hypothesis $\sigma_0 > 1$, the outer solution is $c_{\text{out}}(x) \equiv c_{\text{sat}} = 1$. Since c_{out} automatically satisfies the boundary condition at $x = 0$, a boundary layer develops close to $x = 1$, where c_{xx} must be of $O(\alpha^{-1})$. We can thus look for *inner* solutions by rescaling $c(x,t) = \hat{c}((1-x)/\sqrt{\alpha})$, which proves that the spatial boundary layer has an amplitude of $O(\sqrt{\alpha})$. The function $\hat{c}$ solves an ordinary differential equation independent of α. Figure 3 shows the solution of such equation satisfying the correct boundary conditions $\hat{c}(0) = 0$ and $\lim_{z\to+\infty} \hat{c}(z) = 1$.

4.3 Travelling-wave solution

After a time interval $T(1) = \sigma_0^{1/3}$ (see equation (13)), the amount of drug stored in the solid phase at $x = 1$ vanishes, and $s(1,t) = 0$ for all $t \geq T(1)$. From hence on, the boundary layer starts moving towards the inner part of the interval $[0,1]$. In doing so, it leaves behind a region in which $s = 0$, while c obeys a simple homogeneous diffusion equation. This behavior is confirmed by means of numerical simulations, whose results specific to the small diffusion case are reported in Figure 4.

In this section we will derive explicit estimates for quantities of applicative interest. In particular, we will study the speed at which the moving front evolves

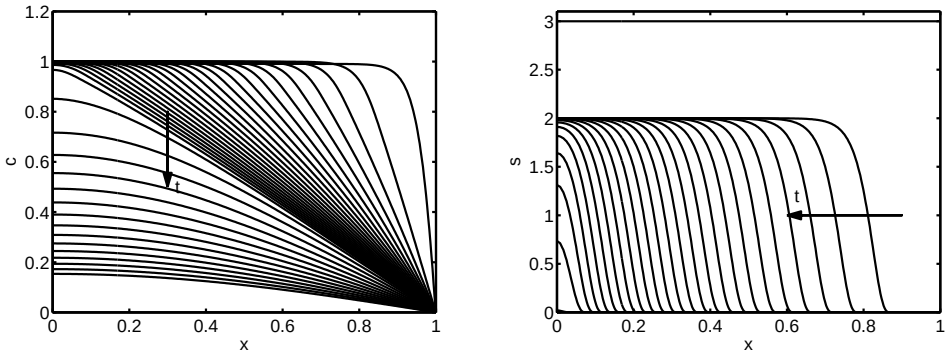

Figure 4: Numerical approximation of the concentrations $c(x,t)$ and $s(x,t)$ at equidistant times when $\alpha = 4.7 \times 10^{-3}$ and $\sigma_0 = 3$.

and we will analyze the behavior of the solutions of the diffusion equation. As a result, we derive how the release rate varies during the evolution of the moving front.

In Proposition 2.3 we have shown that the stopping time T is a strictly monotonically decreasing function of x whenever σ attains a constant value greater than 1, which is the case we are now dealing with. Let then $X(t)$ be the inverse of the function $T(x)$ defined in (8). We seek for solutions of the motion differential equations (2) of the following type

$$s(x,t) = \begin{cases} 0 & \text{if } x > X(t) \\ \varsigma\left(\dfrac{x - X(t)}{\sqrt{\alpha}}\right) & \text{if } X(t) - \Delta < x < X(t) \\ \sigma_0 - 1 & \text{if } x < X(t) - \Delta, \end{cases} \tag{21}$$

$$c(x,t) = \begin{cases} c_{\text{diff}}(x,t) & \text{if } x > X(t) \\ 1 & \text{if } x < X(t), \end{cases}$$

where Δ will turn out to be of $O(\sqrt{\alpha})$ when $\alpha \to 0^+$, and ς and c_{diff} are functions to be determined.

We begin by studying the diffusion problem

$$c_{\text{diff},t} - \alpha c_{\text{diff},xx} = 0, \quad \text{with} \quad c_{\text{diff}}(1,t) = 0 \quad \text{and} \quad c_{\text{diff}}(X(t),t) = 1. \tag{22}$$

More precisely, we seek for self-similar solutions of the form

$$c_{\text{diff}}(x,t) = \gamma\left(\frac{1-x}{1-X(t)}\right), \qquad \gamma(0) = 0, \quad \gamma(1) = 1, \tag{23}$$

where γ is a (positive) function to be determined. The speed at which the front evolves can be determined by a simple mass-balance argument. Indeed, the

amount of drug stored in the whole system at any time t is given by

$$Q(t) = \left[(\sigma_0 - 1)\big(X - \Delta\big) + \int_{X-\Delta}^{X} \varsigma \, dx\right] + \left[X + \int_{X}^{1} \gamma \, dx\right],$$

where the terms within the brackets respectively correspond to the amount of drug stored in the solid, and in the liquid phase. The time derivative of Q must be balanced by the release rate. After a change of variables from x to $z = (1-x)/(1-X)$ in the last integral, we obtain

$$\dot{Q} = \sigma_0 \dot{X} - \dot{X} \int_0^1 \gamma(z) \, dz.$$

Therefore, the motion law for the front turns out to be

$$\left(\sigma_0 - \int_0^1 \gamma(z) \, dz\right) \dot{X} = -\frac{\alpha \gamma'(0)}{1-X} \tag{24}$$

which, incidentally, shows that the correct time scaling is given by α^{-1}, as it could be already guessed from equation (22). The right-hand side of equation (24) provides the release rate

$$R(t) = -\alpha c_x(1,t) = \frac{\alpha \gamma'(0)}{1-X}. \tag{25}$$

Even before having determined γ, equation (25) shows that the release rate is a decreasing function of time. Indeed, the numerator $\alpha\gamma'(0)$ is constant, while the denominator $1 - X$ increases while the front proceeds to the left.

If we now replace (23) in (22), and we make use of (24), we obtain

$$\gamma'' + 2\beta^2 z \gamma' = 0, \tag{26}$$

where

$$\beta^2 = -\frac{\dot{X}(1 - X(t))}{2\alpha} = \frac{\gamma'(0)}{2(\sigma_0 - \int_0^1 \gamma(z) \, dz)}. \tag{27}$$

is a positive self-consistent parameter to be determined in order to quantify the correct speed for the moving front. Equation (26) is to be solved with the boundary conditions $\gamma(0) = 0$, $\gamma(1) = 1$. The solution is given by

$$\gamma(z) = \frac{\operatorname{erf}(\beta z)}{\operatorname{erf}(\beta)}, \tag{28}$$

where erf denotes the error function. Once we replace the solution (28) into the consistency condition (27) we obtain the following implicit condition which determines β:

$$\frac{\mathrm{e}^{-\beta^2}}{\beta\sqrt{\pi}\operatorname{erf}(\beta)} = \sigma_0 - 1. \tag{29}$$

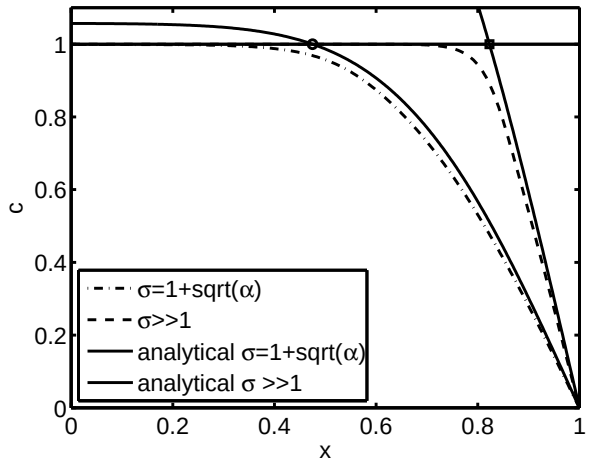

Figure 5: The profiles of $c_{\text{diff}}(x,t)$ for $\sigma_0 = 3$, $\beta = 0.46$ (top, continuous line) and $\sigma_0 = 1+\sqrt{\alpha}$, $\beta = 1.36$ and $t = 15$ (bottom, continuous line) compared with the corresponding profiles obtained with numerical simulations ($\sigma_0 = 3$ dashed line and $\sigma_0 = 1+\sqrt{\alpha}$ dash-dotted line).

Equation (29) cannot be solved analytically in closed form, but its roots can be approximated by means of numerical algorithms for the solution of nonlinear equations. For $\sigma_0 = 3$ we find $\beta = 0.46$ while for $\sigma_0 = 1+\sqrt{\alpha}$ we obtain $\beta = 1.36$. In the first case, *i.e.* for small values of β, the function $\gamma(z)$ is closely approximated by the identity function in the interval $(0,1)$. For larger values of β, $\gamma(z)$ becomes remarkably concave with $\gamma(z) \geq z$ in $(0,1)$. This behavior directly influences the profile of $c_{\text{diff}}(x,t)$ defined in (23). The different graphs of $c_{\text{diff}}(x,t)$ for $t = 15$, $\sigma_0 = 3$, $\beta = 0.46$ and $\sigma_0 = 1+\sqrt{\alpha}$, $\beta = 1.36$ are reported in Figure 5 and compared with the corresponding plots of $c(x,t)$ approximated by means of numerical simulations. Such plots confirm the aforementioned role of function $\gamma(z)$ in shaping the boundary layer profile of the concentration c. Indeed, for large values of σ_0 such profile is almost linear, while it assumes a more rounded shape for smaller σ_0.

Figure 6 shows how β depends on the initial load σ_0. The value of β determines the speed through the relation $\dot{X} = -2\alpha\beta^2/(1-X)$, whose solution is $X(t) = 1 - 2\sqrt{\alpha\beta^2(t-t_0)}$. Such estimates of $X(t)$ and $\dot{X}(t)$ are compared in Figure 7 with the corresponding quantities computed by means of numerical simulations. Figure 7 (left) shows that the analytical and numerical approximations of $X(t)$ differ by an almost constant quantity, which is the error that is accumulated when the traveling wave starts its propagation. This interpretation is confirmed by Figure 7 (right), which highlights that the analytical approach provides an accurate approximation of the travelling wave speed in the middle of its path $0 < X < 1$, while approaching the extrema $X = 0$ and $X = 1$,

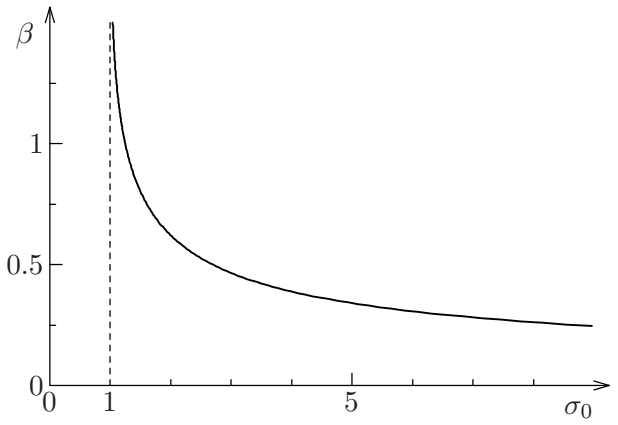

Figure 6: Plot of the solutions of equation (29).

the presence of the boundary conditions affect the accuracy of the first order analytical estimate.

Furthermore, it is interesting to check the asymptotic behavior of β (and, thus, the speed) both when σ_0 is very large, and when it is close to 1. We obtain

$$\beta^2 \approx -\log(\sigma_0 - 1) - \frac{1}{2}\log\big(-\log(\sigma_0 - 1)\big) \qquad \text{as} \quad \sigma_0 \to 1^+$$
$$\beta^2 \approx \frac{1}{2\sigma_0} + \frac{1}{3\sigma_0^2} + O(\sigma_0^{-3}) \qquad \text{as} \quad \sigma_0 \to +\infty.$$

Though solution (28) has been obtained only in terms of an error function, it is worth to be noticed that a quite remarkable approximation to the actual solution can be obtained by simply setting $\gamma_{\text{appr}}(z) = z$. Indeed, it is evident that γ_{appr} satisfies the boundary conditions both in $z = 0$ and in $z = 1$. To obtain a quantitative estimate of the quality of this approximation, we have computed the H^2-relative distance between γ and γ_{appr}, that is $\mathrm{D}(\sigma_0) = \|\gamma - \gamma_{\text{appr}}\|_{H^2} \,/\, \|\gamma\|_{H^2}$. We remark that a small H^2-error implies that both γ and γ' are well approximated by their counterparts γ_{appr} and γ'_{appr}. D can be computed and turns out to be a decreasing function of σ_0. To provide a more precise estimate, we report that $\mathrm{D}(\sigma_0) < 10^{-1}$ for any $\sigma_0 > 2$. If we replace γ with γ_{appr} in (27) we obtain a quite precise analytical estimate of the speed of the moving front

$$\dot{X}_{\text{appr}} = \frac{-\alpha}{(\sigma_0 - \frac{1}{2})(1 - X(t))} \quad \text{whenever } \sigma_0 \gtrsim 2. \tag{30}$$

We now focus attention on the function ς, which provides shape of the wave which propagates, while melting the solid phase into the fluid solution. In order to obtain analytical information of the shape of the moving front, we make resort to the equivalent formulation provided in equation (5). More precisely, we seek

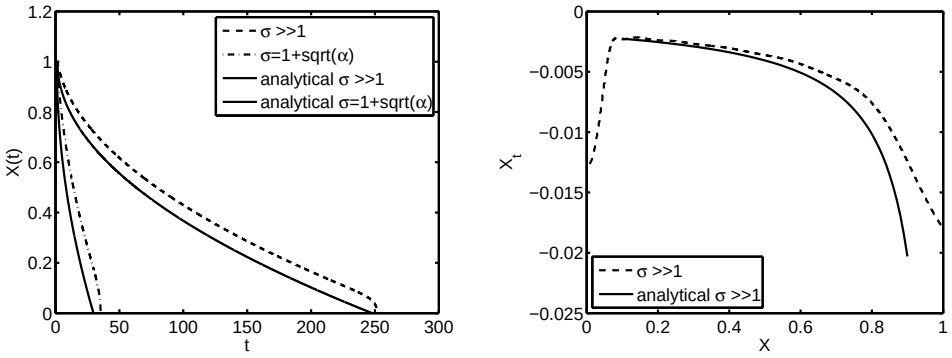

Figure 7: On the left we compare the numerical (dashed) and analytical (continuous) approximations of the vanishing point of concentration s, denoted with $X(t)$. The two sets of curves correspond to $\sigma_0 = 3$, $\beta = 0.46$ (continuous, top) and $\sigma_0 = 1 + \sqrt{\alpha}$, $\beta = 1.36$ (continuous, bottom). On the right, for $\sigma_0 = 3$ and $\beta = 0.46$ is reported the comparison between the numerical approximation of $\dot{X}$ versus X (dashed) with the corresponding analytical estimate $\dot{X} = -2\alpha\beta^2/(1 - X)$ (continuous).

solutions of the form

$$u(x,t) = \varrho\left(\frac{x - X(t)}{\sqrt{\alpha}}\right).$$

Were these solutions to be found, we would immediately obtain from them $\varsigma = (\varrho^+)^3$, and $c = 1 + u_t$. We remark that, since $u_t = -\varrho'\dot{X}/\sqrt{\alpha} = O(\sqrt{\alpha})$ by virtue of (24), we prove that $c \approx 1$ in the moving front, as we implicitly assumed in (21).

If we let $z := (x - X)/\sqrt{\alpha}$, we obtain that ϱ must obey the ordinary differential equation

$$\varrho'' = (\varrho^+)^3 - (\sigma_0 - 1) \tag{31}$$

We seek for solutions of equation (31) such that $\varrho(0) = 0$, and $\lim_{z\to-\infty} \varrho(z) = (\sigma_0 - 1)^{1/3}$. This latter condition ensures that, when $(X - x) \gg \sqrt{\alpha}$, ϱ approaches the value $(\sigma_0 - 1)^{1/3}$, which is equivalent to say that ς approaches the value $\sigma_0 - 1$. We further remark that, since we are only interested in the descent of ϱ towards its null value (attained at $x = X$), we can safely drop the positive part from the term $(\varrho^+)^3$ in (31). A first integration of the equation thus obtained provides

$$\varrho'^2 = \frac{1}{2}(y - \varrho)^2(\varrho^2 + 2y\varrho + 3y^2), \tag{32}$$

where we have introduced the notation $y = (\sigma_0 - 1)^{1/3}$. Equation (32) turns out to be integrable as well, and we obtain the analytical expression of the shape of

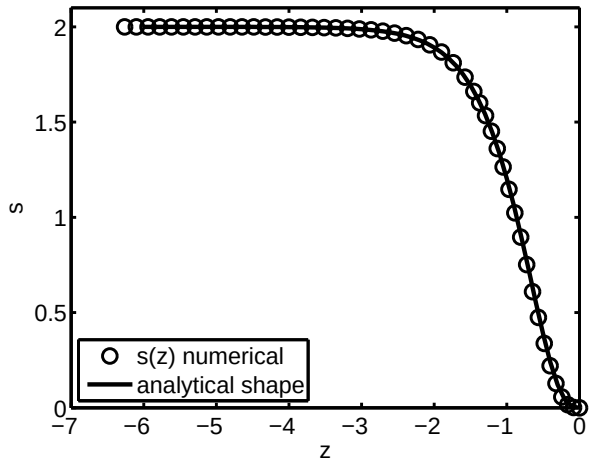

Figure 8: Numerical (dots) and analytical (continuous) approximations of the travelling wave solution for the case $\sigma_0 = 3$, $\beta = 0.46$.

the moving front

$$\varrho(z) = \varsigma(z)^{1/3} = y(1 - \mathrm{e}^{\sqrt{3}zy}) \left(1 - \frac{\mathrm{e}^{\sqrt{3}zy}(7 + 6\sqrt{2} - \mathrm{e}^{\sqrt{3}zy})}{17 + 12\sqrt{2} + \mathrm{e}^{\sqrt{3}zy}(8 + 6\sqrt{2} - \mathrm{e}^{\sqrt{3}zy})} \right).$$

Figure 8 shows the comparison of $\varsigma(z)$ with one of the travelling wave profiles of $s(x,t)$ reported in Figure 4 (right), to which we have applied the linear change of coordiantes $z = (x - X(t))/\sqrt{\alpha}$. Again, this highlights the excellent accuracy of the analytical estimates with respect to numerical approximation of the problem solution.

4.4 Non-uniform and unsaturated loading

Most of the conclusions we have derived in this section remain valid when the initial loading $s(x,0) = \sigma(x)$ is not uniform, provided $\sigma(x) > 1$ for all $x \in [0,1]$. It is in particular easy to show that the initial time evolution is characterized by the melting and the boundary layer in §4.1 and §4.2. Moreover, the moving front described in equations (21)-(25) persists. The speed of the front is still determined by the mass balance (24), though we have to keep in mind that in this case $\dot{X}$ depends on X also through $\sigma(X)$. In particular, with a suitable variable loading it would be possible to obtain a constant speed, independent of the position. Equation (30) suggests that a reasonable approximation to such an initial loading would be given by $\sigma(x) = \frac{1}{2} + \text{const.}(1-x)^{-1}$. Nevertheless, equation (25) shows that a variable initial loading is not sufficient to overturn the monotonically decreasing behavior of the release rate.

We finally consider the case in which the initial loading is not sufficient to reach the saturated state described in §4.1. More precisely, we focus on the opposite situation, in which $\sigma(x) < 1$ for all $x \in [0,1]$. Intermediate cases can then be easily pictured at by collecting the features of both limiting case. In the case of insufficient loading, the initial time evolution drives the system towards the configuration in which $s = 0$, and $c(x,t) = \sigma(x) < 1$ in a dimensionless time t_0 which remains of $O(1)$ when $\alpha \to 0$, that is, in a time in which diffusion can still be neglected. Starting from this configuration, the evolution of the system is driven by the simple diffusion equation

$$c_t - \alpha c_{xx} = 0 \quad \text{in } x \in [0,1], \quad \text{with } c(x,t_0) = \sigma(x),\ c_x(0,t) = 0,\ \text{and } c(1,t) = 0. \tag{33}$$

The differential problem (33) can be solved analytically (see Appendix A for details). Let $\Theta(x,\xi,t)$ be the Green function defined in (39). Then,

$$c(x,t) = \int_0^1 \sigma(\xi)\,\Theta(x,\xi,t)\,d\xi.$$

Because of the superposition principle, it is interesting to analyze the case in which σ is a Dirac-delta function: $\sigma(x) = \delta(x - x_0)$, with $x_0 \in (0,1)$. When this is the case, we have $c(x,t) = \Theta(x,x_0,t)$. In particular the release rate in this regime is given by

$$\begin{aligned} R(t) &= -\alpha c_x(1,t) \\ &= \alpha\pi \sum_{n=0}^{+\infty} (-1)^n (2n+1) \cos\frac{(2n+1)\pi x_0}{2} \exp\left(-\frac{\alpha(2n+1)^2\pi^2(t-t_0)}{4}\right). \end{aligned}$$

Whatever the value of x_0, R turns out to be an increasing function up to a critical time $t_{\max}(x_0)$, after which it decreases monotonically to 0. Therefore, non monotonic release rates can be easily recovered in this regime. Figure 9 shows how the characteristics of the release rate depend on x_0. The left panel exhibits the dependence on x_0 of three characteristic times: the intermediate time $t_{\max}$ is the time at which the release rate attains its maximum; the extreme times $t_{\pm\frac{1}{2}}$ are the times at which the release rate is equal to $\frac{1}{2}$ its maximum value. In other words, $t_{-\frac{1}{2}} < t_{+\frac{1}{2}}$ are the only roots of the equation $R(t_{\pm\frac{1}{2}}) = \frac{1}{2}R(t_{\max})$. The difference $t_{+\frac{1}{2}} - t_{-\frac{1}{2}}$ increases when x_0 departs from the extreme $x = 1$. This fact shows that the release of the drug is more concentrated in time whenever one chooses to place x_0 close to the boundary $x = 1$. This fact is confirmed by the right panel in Figure 9, where the maximum value $R(t_{\max})$ is plotted against x_0.

4.5 Towards an optimal design problem

It is the aim of this final section to investigate whether and how a non-uniform initial solid concentration profile can help in obtaining a target pattern of the

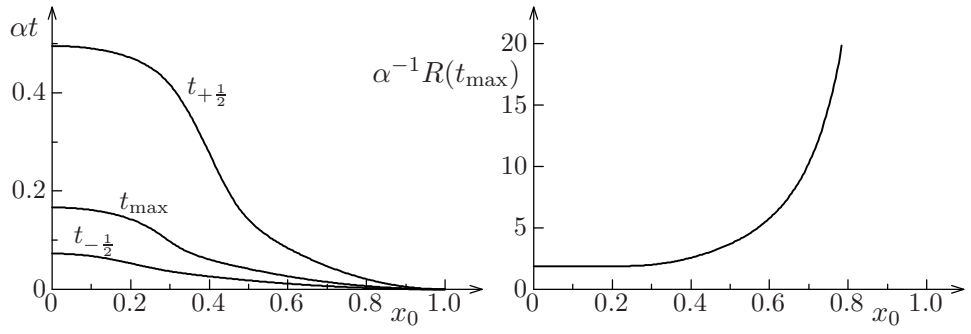

Figure 9: Qualitative properties of the release rate in case of insufficient loading. The times $t_{\max}$ and $t_{\pm\frac{1}{2}}$ are defined in the text.

release rate. The final goal is clearly to move a step towards setting up a control problem capable to deliver a prescribed release profile by suitably choosing the profile $\sigma(x)$.

First of all, we observe that in the case of non uniform solid concentration profile, problem (5) should be replaced by (6), because it allows us to consider fully discontinuous and piecewise vanishing functions $\sigma(x)$. We consider a test case where $\sigma(x)$ resembles a piecewise constant function in $(0, 1)$. More precisely $\sigma(x) = 3$ in $(0, 0.4)$, $\sigma(x) = 0$ in $(0.4, 0.8)$, $\sigma(x) \simeq 1 + \sqrt{\alpha}$ in $(0.8, 0.1)$.

The present test case is designed with the aim of obtaining a possibly increasing release rate over time. This is the purpose of the initially moderate drug charge ($\sigma = 1 + \sqrt{\alpha}$) in proximity of the release point $x = 1$, followed by a significant drug burst ($\sigma = 3$ in $(0, 0.4)$) that will be released in a second phase, because of the delay needed to reach the rightmost side of the domain.

The results provided by numerical simulations of the non-uniform initial solid concentration problem show however that this intuitive belief is not trivial to achieve. Indeed, the computed release rate profiles turn out to be monotonically decreasing with time, as depicted in Figure 10.

Even though not immediately intuitive, this result can be justified by means of the previous analysis. The drug release process can be subdivided in three steps. In the initial step, only the rightmost part of drug is being released, and the release rate, which is initially singular, quickly decreases until a plateau is reached. In this initial phase, the liquid drug concentration $c(x, t)$ in proximity of the point $x = 1$ increases, but its derivative $c_x(1, t)$ does not. This fact is illustrated in Figure 11 (top left). In the second phase, Figure 11 (middle), according to the fact that the solid concentration $s(x, t)$ is almost vanishing in $(0.4, 1)$, the liquid concentration in this region migrates towards a profile that is almost linear and constant in the remaining part of the domain. This process further reduces the release rate. Finally, in the third phase, a travelling wave solution is established, as clearly shown by Figure 11 (bottom right).

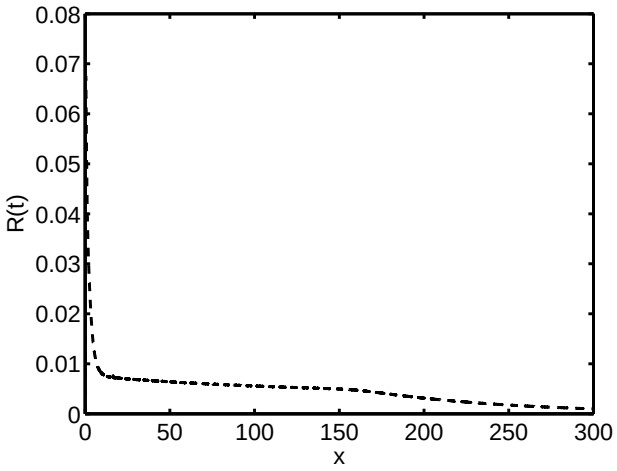

Figure 10: Numerical approximation of the release rate profile $R(t)$ for the non-uniform initial solid concentration problem.

5 Conclusions

In this paper we have investigated a two-phase model for the drug delivery in biomedical devices. The model accounts for the possibility of loading the drug in its solid phase in a non-uniform pattern, represented by a variable initial distribution in an interval, which mimics the substrate, typically a polymeric mixture, releasing the drug. During the evolution, the solid drug melts in a surrounding fluid, in which it diffuses until it reaches the end of the interval, where the drug is delivered.

We have studied both the analytical properties of the solution of the coupled differential evolution equations, and the features of the numerical solutions of the model. In particular, we have traced the properties of the *stopping time*, defined as the (position-dependent) time at which the solid drug is completely melted, and of the *release rate*, at which the drug is delivered through one end of the interval.

General analytical estimates allow to prove that the stopping time is finite, and suitable bounds (which turn out to be quite sharp in the large diffusion limit) are derived in Section 2. We have then derived two equivalent single-variable problems, which allow to replace the original system by a single partial differential equation, whose solution determines the properties of both the solid and fluid drug concentrations. Finally (see Proposition (2.3)) we have shown that the stopping time is a strictly monotonically decreasing function of position for a wide class of initial loadings, including uniform loadings.

The large-diffusion limit has allowed us to obtain quite precise analytical information on the solutions. It is a regular perturbation problem, and precise

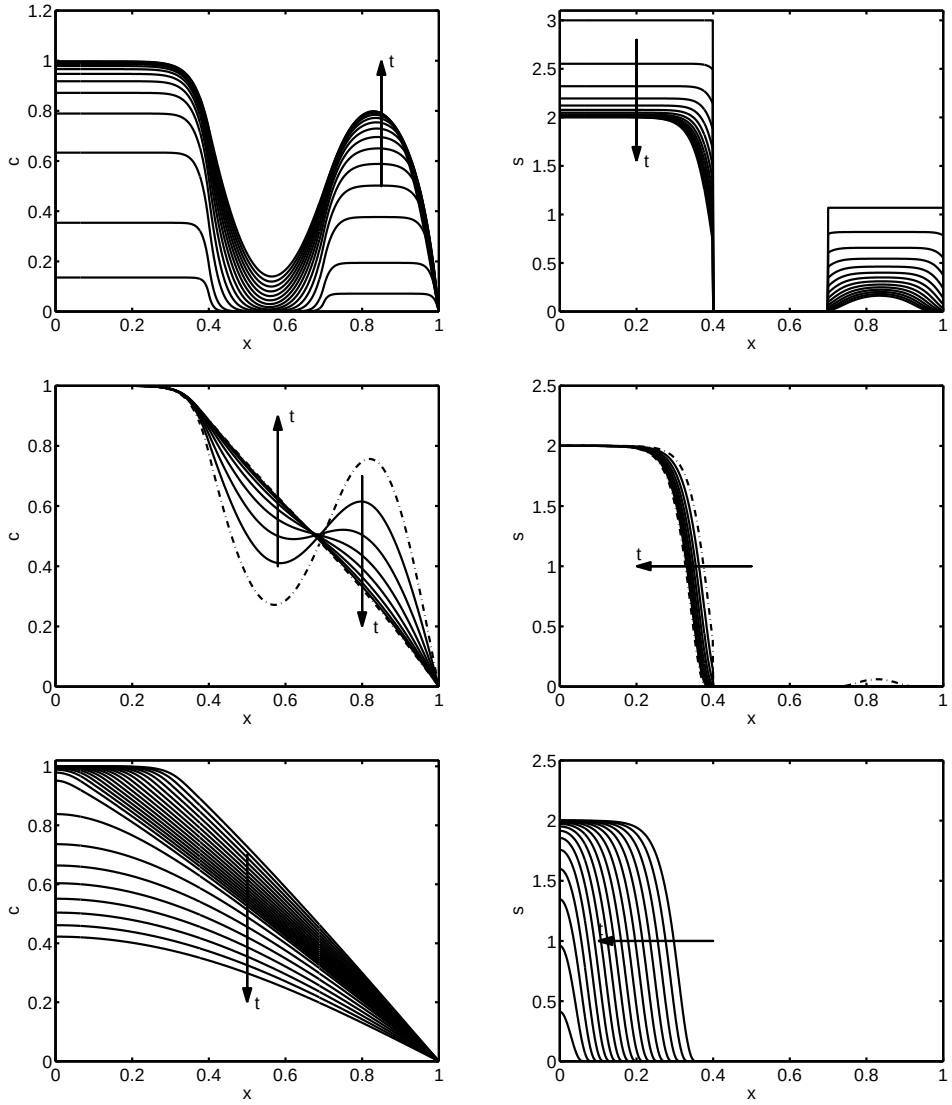

Figure 11: Numerical approximation of liquid concentration $c(x,t)$ (left) and the solid concentration $s(x,t)$ (right) for the test-case described in the text, at different phases of the release process. In particular, the initial phase $t \in (0, 1.3)$, the intermediate phase $t \in (2, 10)$ and the final phase $t \in (20, 200)$ are reported from top to bottom.

estimates for both the stopping time (see equation (15)) and the release rate (see equation (16)) are provided.

The small-diffusion limit is far more complicated, as it gives rise to a singular perturbation problem. We have been able to identify and describe the fast time evolution, which develops a boundary layer close to the outer end of the device. At longer time scales, a travelling-wave solution emerges. Such solution is peculiar, since it preserves the shape while it propagates, but its velocity is position-dependent (see equation (24)). By studying the unsaturated loading in this regime, we have provided an explicit example of how it is possible (though not easy) to envisage release rates which are not monotonically decreasing with time.

This paper is intended to set up and analyze the model in which the following optimal control problem is to be studied: *Given a prescribed time-pattern for the release rate, determine the profile of a possibly non uniform $\alpha(x)$, and the spatial pattern of the initial loading which guarantees the desired release.* Such an optimal problem will be the focus of future studies, though the results of the present study suggest that some generalizations of the model could help in achieving the goal. First of all, one could trace the dynamics of the device as well, in order to account for biodegradable devices, which melt themselves during the time evolution. Moreover, experimental results suggest that the diffusion, that we have taken as a fixed constitutive parameter, could depend on the properties of the device, and more specifically on the amount of solid drug still to be melted.

A Analytical tools

A.1 A maximum principle

Lemma A.1 *Let $\gamma \in C\left([0,T];L^1(0,1)\right)$ and let $f \in C^1\left((0,T];H^1(0,1)\right) \cap C\left([0,T];L^2(0,1)\right)$ satisfy*

$$\partial_t f - \partial_{xx} f + \gamma f \geq 0,$$

with initial condition $f(x,0) \geq 0$, and boundary conditions $\partial_x f(0,t) = 0$, $f(1,t) \geq 0$.

Then $f(x,t) \geq 0$ for every t.

Proof. By assumption we can write $|\gamma(x,t)| \leq k + \gamma_1(x,t)$, where k is constant and $|\gamma_1|_1 < 1$. Let

$$\rho(t) = \frac{1}{2}\int_0^1 |f^-(x,t)|^2\,dx.$$

We obtain that $\rho \in C^1((0,T]) \cap C([0,T])$ and $\rho(0) = 0$. By testing the equation with f^- and integrating by parts we obtain

$$\begin{aligned}\rho'(t) &= -\int_0^1 f^-\partial_t f\,dx \leq -\int_0^1 \left(f^-\partial_{xx} f - \gamma|f^-|^2\right)\,dx \\ &\leq -|\partial_x f^-|_2^2 + k|f^-|_2^2 + |\gamma_1|_1|f^-|_\infty^2 \leq \left(-1 + |\gamma_1|_1\right)|\partial_x f^-|_2^2 + k|f^-|_2^2 \\ &\leq 2k\rho(t)\end{aligned}$$

(recall that, since $f^-(1,t) = 0$, $|f^-|_\infty \le |\partial_x f^-|_2$ for any t). Then we deduce that $\rho(t) \le e^{2k}\rho(0)$ and the lemma follows. □

A.2 Existence and uniqueness of the solution

We now prove that problem (5) has a unique solution, and we obtain further regularity for this solution. In order to comprise the case of a non constant $\sigma = \sigma(x)$, it is convenient to work with the equivalent formulation (6), involving homogeneous boundary conditions. Then, we set

$$v(x,t) = u(x,t) - \sigma^{1/3}(x) + t = \int_0^t c(x,\tau)\,d\tau; \quad s(x,t) = \left[\left(\sigma^{1/3}(x) - t + v(x,t)\right)^+\right]^3,$$

so that v solves the initial-boundary value problem

$$\begin{cases} v_t - \alpha v_{xx} = \sigma - \left[\left(\sigma^{1/3} - t + v\right)^+\right]^3 & \text{in } Q_T \\ v(x,0) = 0 & \text{on } C \\ v_x(0,t) = 0 & \text{on } N \\ v(1,t) = 0 & \text{on } D, \end{cases} \tag{34}$$

where $Q_T = (0,1)\times(0,T)$, $C = [0,1]\times\{0\}$, $N = \{0\}\times[0,T]$, $D = \{1\}\times[0,T]$. By choosing $\sigma^{1/3}$ smooth enough, v has the same regularity properties as u. We now prove:

Proposition A.1 *There exists exactly one solution $v \in C^{2,1}(Q_T) \cap C(\overline{Q_T})$ of (34). Moreover, v satisfies the following regularity properties:*

- *v_t, v_x $v_{tx} \in C(\overline{Q_T})$;*
- *v_{xx}, v_{xxx}, v_{tt} and v_{txx} are continuous in Q_T, uniformly up to N and to $C \cup D\backslash\{(1,0)\}$.*

Proof. We divide the proof into four steps.
1. *A priori bounds.* From the maximum principle (see §A.1) any smooth enough solution v of problem (34) satisfies $v \le v_\sigma$, where v_σ is the solution to the *linear* problem $v_t - \alpha v_{xx} = \sigma$ with the same (homogeneous) initial-boundary conditions. As in the proof of the estimates of Proposition 2.1, we assume that $0 \le \sigma(x) \le \sigma_1$. Then, again by the maximum principle, it is easily verified that $v_\sigma \le \frac{\sigma_1}{2\alpha}(1-x^2)$, so that any solution v to (34) satisfies

$$v(x,t) \le \frac{\sigma_1}{2\alpha}(1-x^2). \tag{35}$$

In particular, it follows that $v_t - \alpha v_{xx} \ge -\sigma_\alpha$ with $\sigma_\alpha = \sigma_1\left[(1 + \frac{\sigma_1^{2/3}}{2\alpha})^3 - 1\right]$; thus, we also have the lower bound

$$v(x,t) \ge -\frac{\sigma_\alpha}{2\alpha}(1-x^2). \tag{36}$$

Finally, by denoting with $f(x,t)$ the term at the right hand side of the equation in (34), we have $-\sigma_\alpha \le f(x,t) \le \sigma$; hence, by standard calculations we get the uniform estimate

$$\|v\|_{L^2((0,T);H^1(0,1))} \le C\sqrt{T} \tag{37}$$

for every solution v.

2. *Local solvability.* Following a classical approach [1], one can reformulate problem (34) as an integral equation; then, we consider the equation

$$v(x,t) = v_\sigma(x,t) - \int_0^t \int_0^1 \Theta(x,\xi,t-\tau) \left[\left(\sigma^{1/3} - \tau + v \right)^+ \right]^3 d\xi d\tau, \tag{38}$$

where v_σ was defined in step 1 and

$$\Theta(x,\xi,t) = 2 \sum_{n=0}^{\infty} e^{-\alpha \left(n+\frac{1}{2}\right)^2 \pi^2 t} \cos\left[\left(n + \frac{1}{2} \right) \pi x \right] \cos\left[\left(n + \frac{1}{2} \right) \pi \xi \right]. \tag{39}$$

Let $V = \{ v \in H^1(0,1),\, v(1) = 0 \}$. We first prove that (38) has a unique solution in the space $\mathcal{C}([0,T];V)$ for T small enough. To this aim, we consider the function

$$S[v](x,t) = s(x,t) = \left[\left(\sigma^{1/3}(x) - t + v(x,t) \right)^+ \right]^3, \quad \text{where } v \in \mathcal{C}([0,T];V). \tag{40}$$

By the smoothness assumptions on $\sigma^{1/3}$ and recalling that v is continuous and bounded, it can be shown that $s \in \mathcal{C}([0,T];H^1(0,1))$. Besides, by (37),

$$\|s\|_{L^2((0,T);H^1(0,1))} \le C\sqrt{T}, \tag{41}$$

with C depending on $\|v\|_{\mathcal{C}([0,T];H^1(0,1))}$. Note that, if the estimates (35) and (36) hold, we can take C independent of v. Finally, we have

$$s(1,t) = \left[\left(\sigma^{1/3}(1) - t \right)^+ \right]^3, \tag{42}$$

so that $0 \le s(1,t) \le \sigma(1)$. Let us define

$$S_n(\tau) = \int_0^1 s(\xi,\tau) \cos\left[\left(n + \frac{1}{2} \right) \pi \xi \right] d\xi \tag{43}$$

and

$$\tilde{S}_n(t) = \int_0^t e^{-\alpha \left(n+\frac{1}{2}\right)^2 \pi^2 (t-\tau)} S_n(\tau)\, d\tau. \tag{44}$$

By denoting with $\Theta S[v](x,t)$ the integral term in (38), we now have

$$\Theta S[v](x,t) = 2 \sum_{n=0}^{\infty} \tilde{S}_n(t) \cos\left[\left(n + \frac{1}{2} \right) \pi x \right] \tag{45}$$

Since $s(\cdot,\tau) \in H^1(0,1)$, we can integrate by parts in (43), obtaining

$$\left(n + 1/2\right) \pi S_n(\tau) = (-1)^n s(1,\tau) - \int_0^1 s_\xi(\xi,\tau) \sin\left[\left(n + \frac{1}{2} \right) \pi \xi \right] d\xi; \tag{46}$$

then, by (42) and by Hölder inequality, we get the bound

$$\left| \left(n + 1/2\right) \pi S_n(\tau) \right| \le \sigma(1) + \frac{1}{2} \|s(\cdot,\tau)\|_{H^1(0,1)}. \tag{47}$$

By further applying Hölder inequality in (44), we finally obtain

$$\begin{aligned}\big(n+1/2\big)\pi\big|\tilde{S}_n(t)\big| &\leq \frac{\sigma(1)}{\sqrt{2\alpha}\big(n+1/2\big)\pi}\sqrt{t}\\ &\quad+\frac{1}{2}\left[\int_0^t e^{-2\alpha\left(n+\frac{1}{2}\right)^2\pi^2(\tau)}\,d\tau\right]^{1/2}\|s\|_{L^2(0,t;H^1(0,1))}\\ &\leq C_1\frac{1}{\big(n+1/2\big)}\sqrt{t}+C_2\frac{\|s\|_{L^2(0,t;H^1(0,1))}}{\big(n+1/2\big)^{1-2\delta}}\,t^{\delta},\end{aligned}\tag{48}$$

for any $\delta>0$. By choosing $0<\delta<1/4$ in the above estimate and by using it in (45), together with (41), it follows that the operator given by the right hand side of (38):

$$v\mapsto v_\sigma-\Theta S[v],$$

maps a ball around v_σ in $\mathcal{C}([0,T];V)$ into itself for T small enough. We are now left with the Lipschitz estimate of $\Theta S[v]$ in $\mathcal{C}([0,T];V)$. By (40) and by standard calculations, we have $\big|S[v_1]-S[v_2]\big|\leq L|v_1-v_2|$, and

$$\big|\big(S[v_1]-S[v_2]\big)_x\big|\leq L_1|(v_1-v_2)_x|+L_2|(v_2+\sigma^{1/3})_x|\,|(v_1-v_2)|,$$

where the constants L, L_1, L_2 only depend on the sup norm of v_1 and v_2. We can now repeat the previous estimates by replacing $S[v](x,t)$ with $\{S[v_1]-S[v_2]\}(x,t)$ (note that $\{S[v_1]-S[v_2]\}(1,t)=0$). Then, we get

$$\begin{aligned}\|\Theta S[v_1]-\Theta S[v_2]\|_{\mathcal{C}([0,t];H^1(0,1))}\leq\big[&M_1\|v_1-v_2\|_{L^2(0,t;H^1(0,1))}\\&+M_2\|v_1-v_2\|_{\mathcal{C}([0,t];H^1(0,1))}\big]t^{\delta},\end{aligned}$$

where the constants M_1, M_2 depend on the sup norm of v_1, v_2 and M_2 also on the $L^2(0,t;H^1(0,1))$ norm of v_2. Note that M_1, M_2 are also uniformly bounded whenever v_1, v_2 satisfy (35), (36) and (37). By the previous discussion and by the fixed point theorem, we conclude that for small enough $T>0$ there exists a unique solution $v\in\mathcal{C}([0,T];H^1(0,1))$ of (38). Moreover, by computing the term by term time derivative of (45) and using again (47) in the estimate of the derivatives of (44), one can show that v is a *weak solution* of (34), in the sense that $v_t\in\mathcal{C}((0,T),V')$ (V' being the dual space of V) and

$$<v',w>+\alpha\int_0^1 v_xw_xdx=\int_0^1\{\sigma-S[v]\}wdx$$

for every $w\in V$ and every time $0<t\leq T$, with $S[v]$ given by (40); by same bound (47) it also follows that v_x is continuous on $\overline{Q}_T$. Next, we are going to show that the solution v has further regularity.

3. *Improved regularity and global solution.*

In order to gain more regularity, it is convenient to exploit a known theorem for weak solutions of parabolic problems [5], chap.7, thm. 5, which applies to v considered as a (weak) solution to the *linear* problem $v_t-\alpha v_{xx}=f(x,t)$, where $f=\sigma-S[v]$ and v is the prevously obtained local solution. By the boundedness of f, the regularity theorem implies $v_t\in L^2((0,T);L^2(0,1))$; then, by direct computation we get $f_t=-S[v]_t\in L^2(0,T;L^2(0,1))$, so that we also have $v_t\in L^\infty((0,T);L^2(0,1))$ by the same theorem.

Thus, by differentiating (43) we find that the term $|S_n'(\tau)|$ is *bounded* in $(0,T)$. Now, by writing the derivative of (44) in the form

$$\tilde{S}_n'(t) = e^{-\alpha\left(n+1/2\right)^2\pi^2 t} S_n(0) + \int_0^t e^{-\alpha\left(n+\frac{1}{2}\right)^2\pi^2(t-\tau)} S_n'(\tau)\, d\tau, \tag{49}$$

the last term is uniformly bounded by $C\,\|S_n'\|_{L^\infty(0,T)}/(n+1/2)^2$. As a consequence, for every $t \in (0,T]$ we can differentiate term by term with respect to t the series at the right side of (45) obtaining a *continuous function*, and further weakly differentiate with respect to x obtaining a function in $L^2(0,1)$; but the same is true for the function v_σ at the right side of (38), so that we conclude:

$$v \in \mathcal{C}^1((0,T]; H^1(0,1)).$$

Now, the solution v has *enough regularity* to apply the maximum principle of appendix 1; hence, by the a priori bounds (35), (36), (37), the estimates obtained for the local existence are uniform (independent of the solution) and global existence follows by standard arguments.

4. *Higher regularity.*

We first prove that $v_t \in \mathcal{C}(\overline{Q}_T)$; note that, by the initial condition, $s(\xi,0) = \sigma(\xi)$. Hence, by evaluating (43) at $\tau = 0$ and by explicit calculations, it follows that

$$2\sum_{n=0}^{\infty} S_n(0) e^{-\alpha\left(n+1/2\right)^2\pi^2 t} \cos\left[\left(n+\frac{1}{2}\right)\pi x\right] = \partial_t v_\sigma(x,t), \qquad \forall\, t>0.$$

Thus, by differentiating (38) with respect to t and taking account of (45) and (49), we get

$$v_t(x,t) = 2\sum_{n=0}^{\infty}\Big[\int_0^t e^{-\alpha\left(n+\frac{1}{2}\right)^2\pi^2(t-\tau)} S_n'(\tau)\, d\tau\Big] \cos\left[\left(n+\frac{1}{2}\right)\pi x\right]. \tag{50}$$

By the estimate following (49), the series (50) converges uniformly in $\overline{Q}_T$, defining a continuous function v_t, with $v_t(1,t) = 0$; hence, by equation (34) (in weak form) we also find that the second derivative v_{xx} is continuous and bounded in Q_T. Note further that $v_t(x,0) = 0$, so that, by the initial condition, we obtain the continuity of v_{xx} in $Q_T \cup C$.

We remark that by the previous analysis it also follows $v_t \in \mathcal{C}([0,T]; H^1(0,1))$; by (40), *the same is true for* s_t, so that we may integrate by parts the expression $S_n'(\tau) = \int_0^1 s_t(\xi,\tau)\cos\left[\left(n+\frac{1}{2}\right)\pi\xi\right] d\xi$ and by estimates similar to those of step 2 (see (46)-(48)) we finally obtain

$$\left(n+1/2\right)\pi\Big[\int_0^t e^{-\alpha\left(n+\frac{1}{2}\right)^2\pi^2(t-\tau)} S_n'(\tau)\, d\tau\Big] \le C\frac{\|s_t(1,\cdot)\|_{\mathcal{C}([0,T])} + \|s_{tx}\|_{\mathcal{C}([0,T];L^2(0,1))}}{\left(n+\frac{1}{2}\right)^2},$$

which proves the continuity of v_{tx} in $\overline{Q}_T$ (take the x derivatives of the terms in (50)); then, $v_{xt} = v_{tx}$.

By collecting the results proved so far, we conclude that $v_x \in W^{1,\infty}(Q_T)$; thus, v_x is *Lipschitz continuous* in $\overline{Q}_T$. Clearly, $v(x,t) = -\int_x^1 v_x(s,t)ds$ is also Lipschitz continuous; moreover, v_t and v_{xx} are continuous in Q_T and v solves problem (34) in the ordinary sense. By denoting as before with $f(x,t) = \sigma(x) - s(x,t)$ the right hand side of the equation in (34), we now have that f and f_x are Lipschitz functions in $\overline{Q}_T$, with

$f(1,0)=0$. By reflection about $x=0$ and by the Neumann condition, we can take v as the solution of the Cauchy-Dirichlet problem

$$\begin{cases} v_t - \alpha v_{xx} = f(x,t) & -1 < x < 1,\ 0 < t < T \\ v(x,0) = 0 \\ v(-1,t) = v(1,t) = 0, \end{cases}$$

where $f(1,0) = f(-1,0) = 0$. We can now apply classical regularity results (interior and up to the boundary, see e.g., [9], chap. 3, sec. 5) to conclude that v_{xx}, v_{xxx}, v_t and v_{xt} are (Hölder) continuous in Q_T, uniformly in every domain whose closure is contained in $\overline{Q}_T \backslash \{(1,0)\}$. But this in turn implies that the same holds for f_t, f_{xx} and f_{xt}; thus, we further deduce that v_{tt} and v_{txx} are continuous in Q_T up to N and to $C \cup D \backslash \{(1,0)\}$.

Finally, uniqueness of the regular solution to problem (34) follows by the Lipschitz continuity of the map $v \mapsto S[v]$ (see [9], chap.7, sect. 4). □

B Numerical approximation of the problem

We briefly summarize here the the numerical approximation techniques that have been applied to obtain the numerical simulations discussed throughout this work.

For simplicity, we refer to the following model problem

$$\begin{cases} u_t - \alpha u_{xx} = g(u) & 0 < x < 1,\ 0 < t < T \\ u(x,0) = u_0(x) \\ u(0,t) = u(1,t) = 0 \end{cases} \tag{51}$$

which corresponds to (5) except from a minor simplification to the boundary conditions that reduces the technical details of the numerical treatment.

We first discretize in space problem (51) by means of Lagrangian finite elements. Given a partition of $(0,1)$ into equidistributed, non-overlapping intervals I_i, $i = 1, \dots, N_h$ of length $h = 1/N_h$, we look for an approximate solution $u_h(t,x) \simeq u(t,x)$ such that

$$u_h(t) \in X^r_{h,0}(0,1) = \big\{ v_h \in C^0([0,1]) \ : v_h|_{I_i} \in \mathbb{P}^r(I_i),\ i = 1, \dots, N_h, \\ v_h(0) = v_h(1) = 0 \big\},$$

being $\mathbb{P}^r(I)$ the space of polynomials of order $r \in \mathbb{N}$ on the interval I. Let $\{\varphi_i(x)\}_{i=1}^{N_h}$ be a Lagrangian basis of $X^r_{h,0}(0,1)$, the problem to determine $u_h(t)$ is then equivalent to find a vector function $U(t) : (0,T) \to \mathbb{R}^{N_h}$ such that

$$\begin{cases} M\dot{U} + AU = G(U),\ 0 < t < T \\ U(0) = U_0 \end{cases} \tag{52}$$

where $U(t) = \{u_i(t)\}_{i=1}^{N_h}$ with $u_h(t,x) = \sum_{i=1}^{N_h} u_i(t)\varphi_i(x)$ and $M, A \in \mathbb{R}^{N_h \times N_h}$ are constant real matrices given by

$$M_{ij} = \int_0^1 \varphi_j \varphi_i dx, \quad A_{ij} = \alpha \int_0^1 \varphi_{x\,j} \varphi_{x\,i} dx$$

and $G(U) : \mathbb{R}^{N_h} \to \mathbb{R}^{N_h}$ is a nonlinear vector function such that

$$G_i(U) = \int_0^1 g(u_h)\varphi_i dx.$$

Provided that $u_0(x) \in L^2(0,1)$, the initial state U_0 can be determined by projection, namely

$$U_0 = \{u_{h,0,i}\}_{i=1}^{N_h} \text{ with } \int_0^1 u_{h,0}\varphi_i dx = \int_0^1 u_0\varphi_i dx,\ i = 1, \ldots, N_h$$

Problem (52) is called semi-discrete and is equivalent to a N_h-dimensional first-order Cauchy problem. We proceed with the time discretization of (52) by means of $(p+1)$-th order ($p = 0, 1, \ldots, 5$) backward differentiation formulae (BDF). Given a sequence of equidistributed times t_n, characterized by a constant time step τ, we look for a sequence of vectors U_n such that

$$MU_{n+1} = M\Big(\sum_{j=0}^{p} a_j U_{n-j}\Big) + \tau b_{-1}\big(G(U_{n+1}) - AU_{n+1}\big) \tag{53}$$

where a_j, b_{-1} are constant coefficients that characterize this family of schemes and are uniquely determined by means of the constraints necessary to reach maximal order of accuracy. For further details we remand to [10].

Problem (53) requires to solve, at each time step, a N_h-dimensional system of nonlinear algebraic equations. Indeed, rearranging the terms of equation (53), we obtain $F(U_{n+1}) = 0$ where $F(V) : \mathbb{R}^{N_h} \to \mathbb{R}^{N_h}$ is

$$F(V) = \big(M + \tau b_{-1}A\big)V - \tau b_{-1}G(V) - M\sum_{j=0}^{p} a_j U_{n-j}$$

The efficient solution of $F(V) = 0$ is not a trivial task. For this purpose, we apply the damped Newton method proposed in [4], which ensure robust and second-order convergence properties. For the sake of clarity, we briefly describe the damped Newton method below. Let $J_F(V)|_{ij} = \partial F_i/\partial V_j$ be the Jacobian matrix relative to $F(V)$. A straightforward computation shows that in our case

$$J_F(U) = \big(M + \tau b_{-1}A\big) - \tau b_{-1}J_G(U), \quad \text{with} \quad J_G(U)|_{ij} = \int_0^1 g'(u_h)\varphi_j\varphi_i dx$$

Then, at the generic time step t_{n+1}, the solution of the problem $F(U_{n+1}) = 0$ is approximated by means of the following algorithm:

1. define $V_0 = U_n$
2. cycle for $k = 0, 1, 2, \ldots$
   (a) find W_{k+1} such that $J_F(V_k)W_{k+1} = -F(V_k)$

(b) define $\lambda_0 = 1$ and E_0 such that $\|E_0\| = 1$

(c) cycle for $m = 0, 1, 2, \ldots$

i. compute $V_{m+1} = V_k + \lambda_m W_{k+1}$

ii. find E_{m+1} such that $J_F(V_k)E_{m+1} = -F(V_{m+1})$

iii. if $\|E_{m+1}\| \leq \min(\|E_m\|, tol)$ then go to (d)
else reduce λ_m (e.g. $\lambda_{m+1} = \lambda_m/2$ and return to (i)

(d) compute $V_{k+1} = V_k + \lambda_m W_{k+1}$

(e) if $\|V_{k+1} - V_k\|/\|V_{k+1}\| \leq tol$ then go to (3)
else return to (a)

3. define $U_{n+1} = V_{k+1}$

The damped Newton algorithm requires to solve at each iteration a linear system of equations defined by the matrix $J_F(V_k)$. This task is achieved by means of direct factorization methods, implemented in the library UMFPACK (see
`http://www.cise.ufl.edu/research/sparse/umfpack`).

The main purpose of numerical simulations in this work, is to provide a reliable comparison term to quantify the efficacy of the analytical estimates that have been derived so far. For this reason, it is important to ensure that the obtained numerical solution correctly capture the behavior of the problem at hand. This is simply achieved by checking the sensitivity of the numerical solution with respect to spatial and temporal resolution parameters, namely h and τ. Let us denote with $u_{h,1}(t,x)$ the numerical solution of (5) obtained by applying the present numerical scheme with linear finite elements ($r = 1$), a mesh characteristic size $h_1 = 1/120$ and a first order BDF scheme ($p = 0$, i.e. forward Euler) with a time step $\tau_1 = 10^{-3}$. Similarly, let $u_{h,2}(t,x)$ be the solution obtained by halving both h and τ, i.e. setting $h_2 = h_1/2$, $\tau_2 = \tau_1/2$. The numerical simulations obtained in the former case can be considered sufficiently accurate provided that the following test is satisfied with a sufficiently small tolerance,

$$\frac{\int_0^T \int_0^1 \left(u_{h,1} - u_{h,2}\right)^2}{\int_0^T \int_0^1 u_{h,1}^2} \leq \text{tol}$$

According to this criterion, the numerical results presented in the previous sections can be considered sufficiently accurate, because they satisfy the previous test with $\text{tol} = 10^{-2}$.

References

[1] J.R. Cannon: *The one-dimensional heat equation*, Addison-Wesley Pub. Co. (Reading, Ma.), 1984.

[2] D.S. Cohen and T. Erneux: *Controlled Drug Release Asymptotics*, SIAM J. Appl. Math. **58** (1998), 1193-1204.

[3] M.C. Delfour, A. Garon, and V. Longo: *Modeling and design of coated stents to optimize the effect of the dose*, SIAM J. Appl. Math. **65** (2005), 858-881.

[4] P. Deuflhard: *A modified Newton method for the solution of ill-conditioned systems of nonlinear equations with application to multiple shooting*, Numer. Math. **22** (1974), 289-315.

[5] L.C. Evans: *Partial differential equations*, (Graduate Studies in Mathematics **19**, AMS) 1998.

[6] L. Formaggia, S. Minisini, and P. Zunino: *Modeling erosion controlled drug release and transport phenomena in the arterial tissue*, to appear on Math. Mod. Meth. Appl. Sci. (M3AS), 2010.

[7] G. Frenning: *Theoretical investigation of drug release from planar matrix systems: effects of a finite dissolution rate*, J. Control. Release **92** (2003), 331-339.

[8] G. Frenning: *Theoretical analysis of the release of slowly dissolving drugs from spherical matrix systems*, J. Control. Release **95** (2004) 109-117.

[9] A. Friedman: *Partial differential equations of parabolic type*, Prentice-Hall, Inc. (Englewood Cliffs, N.J.) 1964.

[10] E. Hairer and G. Wanner: *Solving ordinary differential equations II*, Springer Series in Computational Mathematics **14**, Springer-Verlag, Berlin, 2nd ed., 1996.

[11] T. Higuchi: *Rate of release of medicaments from ointment bases containing drugs in suspension*, J. Pharm. Sci. **50** (1961), 874-875.

[12] T. Higuchi: *Mechanisms of sustained action medication: theoretical analysis of the rate of release of solid drugs dispersed in solid matrices*, J. Pharm. Sci. **52** (1963), 1145-1149.

[13] R. Langer: *New methods of drug delivery*, Science **249** (1990), 1527-1533.

[14] P. Macheras and A. Iliadis: *Modeling in biopharmaceutics, pharmacokinetics, and pharmacodynamics*, Interdisciplinary Applied Mathematics **30**, Springer, New York, 2006.

[15] S.N. Rothstein, W.J. Federspiel, and S.R. Little: *A unified mathematical model for the prediction of controlled release from surface and bulk eroding polymer matrices*, Biomaterials **30** (2009), 1657-1664.

[16] J.S. Soares and P. Zunino: *A mixture model for water uptake, degradation, erosion and drug release from polydisperse polymeric networks*, Biomaterials **31** (2010), 3032-3042.

[17] C. Vergara and P. Zunino: *Multiscale boundary conditions for drug release from cardiovascular stents*, Multiscale Model. Simul. **7** (2008), 565-588.

[18] P. Zunino, C. D'Angelo, L. Petrini, C. Vergara, C. Capelli, and F. Migliavacca: *Numerical simulation of drug eluting coronary stents: mechanics, fluid dynamics and drug release*, Comput. Meth. Appl. Mech. Eng. **198** (2009), 3633-3644.

MOX Technical Reports, last issues

Dipartimento di Matematica "F. Brioschi",
Politecnico di Milano, Via Bonardi 9 - 20133 Milano (Italy)

11/2010 Paolo Biscari, Sara Minisini, Dario Pierotti, Gianmaria Verzini, Paolo Zunino:
Controlled release with finite dissolution rate

10/2010 Alfio Quarteroni, Ricardo Ruiz Baier:
Analysis of a finite volume element method for the Stokes problem

09/2010 Laura M. Sangalli, Piercesare Secchi, Simone Vantini, Valeria Vitelli:
Joint Clustering and Alignment of Functional Data: an Application to Vascular Geometries

08/2010 Francesca Ieva, Anna Maria Paganoni:
Multilevel models for clinical registers concerning STEMI patients in a complex urban reality: a statistical analysis of MOMI^2 survey

07/2010 Laura M. Sangalli, Piercesare Secchi, Simone Vantini, Valeria Vitelli:
Functional clustering and alignment methods with applications

06/2010 Jordi Alastruey, Tiziano Passerini, Luca Formaggia, Joaquim Peiró:
The effect of visco-elasticity and other physical properties on aortic and cerebral pulse waveforms: an analytical and numerical study

05/2010 Matteo Longoni, A.C.I. Malossi, Alfio Quarteroni, Andrea Villa:
A complete model for non-Newtonian sedimentary basins in presence of faults and compaction phenomena

04/2010 Marco Discacciati, Paola Gervasio, Alfio Quarteroni:
Heterogeneous mathematical models in fluid dynamics and associated solution algorithms

03/2010 P.E. Farrell, Stefano Micheletti, Simona Perotto:
A recovery-based error estimator for anisotropic mesh adaptation in CFD

02/2010 Pietro Barbieri, Niccolo' Grieco, Francesca Ieva, Anna Maria Paganoni and Piercesare Secchi: *Exploitation, integration and statistical analysis of Public Health Database and STEMI archive in Lombardia Region*